ANTIMICROBIAL AGENTS AND CHEMOTHERAPY, Oct. 2005, p. 4085–4092 Vol. 49, No. 10
0066-4804/05/$08.00+0 doi:10.1128/AAC.49.10.4085–4092.2005

Atomic Force Microscopy Study of the Effect of Antimicrobial Peptides on the Cell Envelope of *Escherichia coli*

M. Meincken,[1] D. L. Holroyd,[2] and M. Rautenbach[2]*

UNESCO Associated Centre for Macromolecules, Department of Chemistry, University of Stellenbosch, Private Bag X1, Matieland 7602, South Africa,[1] and BIOPEP Peptide Group, Department of Biochemistry, University of Stellenbosch, Private Bag X1, Matieland 7602, South Africa[2]

Received 17 February 2005/Returned for modification 18 March 2005/Accepted 20 June 2005

The influences of the antibacterial magainin 2 and PGLa from the African clawed frog (*Xenopus laevis*) and the hemolytic bee venom melittin on *Escherichia coli* as the target cell were studied by atomic force microscopy (AFM). Nanometer-scale images of the effects of the peptides on this gram-negative bacterium's cell envelope were obtained in situ without the use of fixing agents. These high-resolution AFM images of the surviving and intact target cells before and after peptide treatment showed distinct changes in cell envelope morphology as a consequence of peptide action. Although all three peptides are lytic to *E. coli*, it is clear from this AFM study that each peptide causes distinct morphological changes in the outer membrane and in some cases the inner membrane, probably as a consequence of different mechanisms of action.

Bacterial resistance to conventional antibiotics has become a major problem worldwide, and certain strains of bacteria are already resistant to all available drugs (3, 29). The development of a new family of antibiotics is therefore an important research topic. Antimicrobial peptides are considered good candidates for the next group of antibiotics because their proposed mode of action is different from those of conventional antibiotics (12, 25). To advance antimicrobial peptides to the status of a new group of antibiotics, it is important to understand the mechanisms of action of these agents and the reason for their selectivity against microbes. In this study we compared the actions of three different peptides, namely, melittin, the toxic and hemolytic 26-residue peptide from the European honeybee *Apis mellifera* (6, 11), and two antibacterial peptides from the African clawed frog *Xenopus laevis*, an amide analogue of the 23-residue magainin 2 (32, 33) and the 21-residue PGLa (28), on the membrane of *Escherichia coli*. All three peptides are cationic α-helical antimicrobial peptides with markedly different sequential distributions of polar and nonpolar amino acids. However, all three peptides are amphipathic and highly membranolytic, with PGLa and magainin 2 having a better selectivity, via electrostatic discrimination, toward prokaryotic cells (13, 22) than the hemolytic melittin (which is a nonselective lytic peptide).

Model membrane studies have provided a good understanding of antimicrobial peptides and their mechanisms of action. Different models for the interaction of a peptide with the bacterial membrane have been proposed: the barrel stave model (2), the toroidal pore or wormhole model (5, 31), the carpet model (23), and the peptide aggregate model (19, 30). Most antimicrobial peptides are thought to follow the toroidal pore model and/or carpet model and not the barrel stave model, in which the peptides in the pore need to span the membrane without deformation of the lipid bilayer. Peptides that form toroidal pores remain associated with the phospholipid head groups and insert perpendicularly to the membrane plane by causing the lipid bilayer to fold back on itself. It has been proposed that both melittin (31) and magainin (16, 20) form this type of lytic pore. A second proposal for the mechanism of action of magainin has been the carpet model (23), where peptides cover the membrane like a carpet and remain in a parallel or a surface state. With this model the destruction of the bilayer occurs by the formation of toroidal pores, micelles, and vesicles. At this stage no clear mode of action has been proposed for PGLa, but it is possible that it also follows the toroidal pore model. The aggregate model proposes that micelle-like aggregates of peptides form in the membrane. This disrupts the membrane's permeability and may eventually lead to cell lysis (19, 30). All of these models have been proposed from model membrane studies, which are limited by the absence of many of the biological features found in natural membranes, which, in turn, may influence the interaction with antimicrobial peptides.

In this study, atomic force microscopy (AFM) was used for the analysis of the membranolytic effects in the mechanisms of action of the three antimicrobial peptides by using *E. coli* cells as the live bacterial target. The main advantage of AFM is the possibility of visualization of live cells in situ, which makes it a powerful and very useful technique for the study of the mechanisms of action of antimicrobial peptides on bacterial target cells. Only a few AFM studies have been done on the effect of membrane-active compounds on bacteria, but none of these have addressed the effects of antimicrobial peptides on bacterial surfaces. Braga and Ricci (4) studied the surface alterations of *E. coli* induced by different concentrations of the beta-lactam antibiotic cefodizime by AFM. They found different forms of cell damage, ranging from the formation of holes in the outer membrane to complete lysis of the bacterium. The effect of rare earth metals, such as La^{3+}, on *E. coli* was ob-

* Corresponding author. Mailing address: Department of Biochemistry, University of Stellenbosch, Private Bag X1, Matieland 7602, Republic of South Africa. Phone: 27-21-8085872. Fax: 27-21-8085863. E-mail: mra@maties.sun.ac.za.

served by Liu et al. (15). They also observed substantial surface alterations caused by the replacement of Ca^{2+} with La^{3+}, which led to damage of the cell's outer membrane. Sharma et al. (26) reported on the alterations (a considerable increase in surface corrugation [roughness] and cell lysis) of the cell morphology of *E. coli* after treatment with RISUG (reversible inhibition of sperm under guidance), a polymeric drug with antimicrobial properties. This paper presents the first report on visualization of the influence of antimicrobial peptides on a bacterium by AFM.

MATERIALS AND METHODS

Preparation of peptides. The peptides PGLa and magainin 2 amide (Mag 2a) were synthesized by using the 9-fluorenylmethoxy carbonyl-based solid-phase peptide synthesis methodology (BioSyn). The peptides were purified to >95% purity by using semipreparative reverse-phase (C_{18}) high-performance liquid chromatography. Melittin was purchased from Sigma-Aldrich (Steinheim, Germany). All peptides were analyzed for purity and chemical integrity by electrospray mass spectrometry. The results of electrospray mass spectrometry for melittin showed a high purity and a lack of protein substances, i.e., phospholipases. The peptides were freeze-dried in 50% acetonitrile to ensure sterility. All glassware used in this study was washed thoroughly and pyrolyzed for 1 h at 550°C in order to ensure that they were sterile and detergent-free.

Preparation of bacterial cells. A culture of *E. coli* HB101 was grown overnight at 37°C in nutrient-rich medium, Bacto tryptone soy broth, to late mid-log phase (0.85 ± 0.1 optical density units at 620 nm). The cells in 1.0 ml culture were isolated by centrifugation (1 min in a Pico-Fuge) and washed twice with 1 volume of sterile analytical-grade water. Afterwards, the cells were gently resuspended in water. A small volume of peptide was added to the cells to yield a 25% ± 5% (low peptide concentration) or a 70% ± 10% (high peptide concentration) decrease in the original optical density. The high concentration was thus in effect above the concentration that would cause 50% lysis (50% lethal concentration [LC_{50}]) of the target cell and the low concentration was less than the LC_{50}. The control samples were not treated with peptide.

For AFM analysis the samples were applied on a freshly cleaved mica surface and allowed to dry for about 5 min before imaging. To determine the effect of the peptide on the cell membrane and to ensure that the imaged damage was really due to the peptide, an average of five individual bacterial cells was imaged for every peptide concentration. Analysis was also done with duplicate cultures for each peptide.

The peptide-treated samples were imaged within 30 min after addition of the peptide. In order to locate the bacteria on the substrate, a built-in microscope with a ×300 magnification was used. The images were obtained in air and in tapping mode by using a multimode AFM from Veeco with a scanner with a maximum scan range of 10 by 10 μm. All images were obtained with a scan speed of 0.7 Hz and a resolution of 512 by 512 pixels. A silicon noncontact low-resonance-frequency cantilever from Nanosensors with a resonance frequency of about 160 kHz and a spring constant of about 50 N/m was used. Every scan resulted in a topography image and a phase image, which were acquired simultaneously. Height and size information were acquired with the imaging software from Veeco. The average surface roughness (R_a) was calculated as the arithmetic average of the absolute values of the surface height deviations measured from the plane: $R_a = 1/n \sum_{i=1}^{n} | Z_i |$, where n is the number of measurements (numbered from $i = 1$ to $i = n$) and Z is the height measurement. The height scale is given for each topology image; and the height is depicted as shades of gray, with white being nearest the tip and black being the farthest away in the topology image. An elasticity (or rigidity) scale is given for each phase image; and elasticity is depicted as shades of gray, with white being the most elastic and black being the most rigid.

RESULTS

Images of untreated *E. coli* HB101 cells revealed a relatively smooth surface with no ruptures or large pores. The average surface corrugation (roughness) of an untreated *E. coli* cell was determined to be 2.41 ± 1.37 nm. We determined the average length of an untreated *E. coli* cell to be 3.73 ± 0.75 mm and the average width to be 1.18 ± 0.29 mm, which is somewhat longer than but in accordance with the dimensions of *E. coli* cell size cited in the literature (10). Figure 1A and B shows the topography image and phase image, respectively, of a typical untreated *E. coli* cell. Figure 1C is a magnification of the surface, and it can be seen that the surface membrane is structured to a certain degree but that it shows no grooves or indentations.

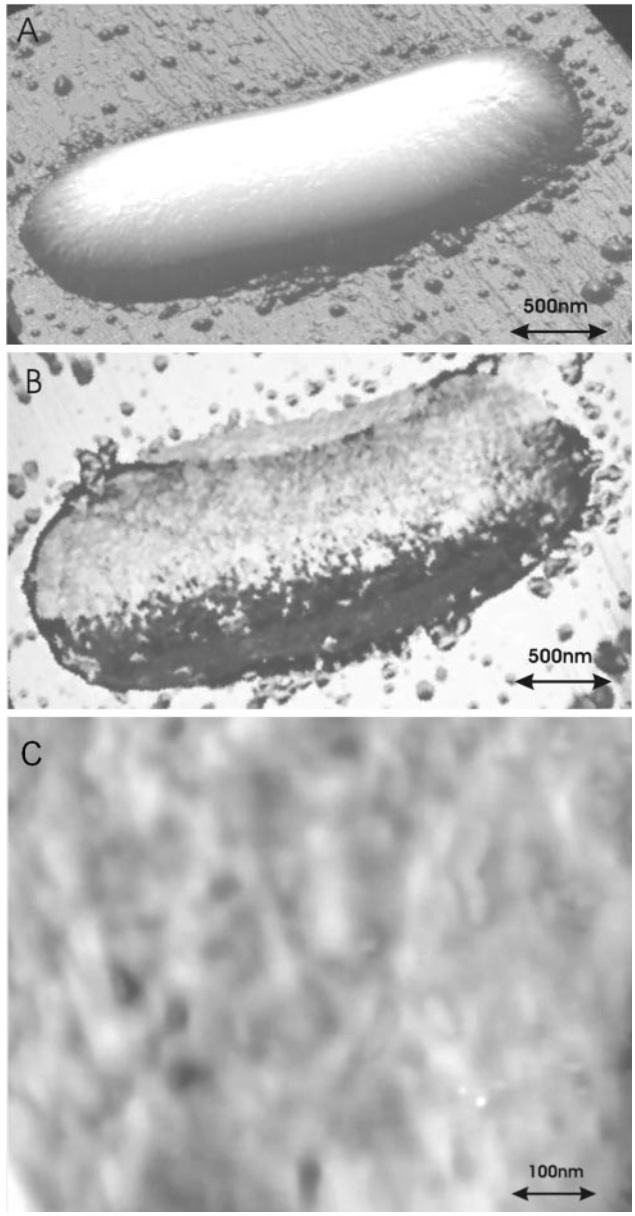

FIG. 1. (A) Topography images and (B) phase images of an untreated *E. coli* cell; (C) magnification of the surface. The color *z* scale ranges from 0 to 1 μm in panel A and from 0 to 90° in panel B.

AFM images were acquired at concentrations greater than and less than the LC_{50} for each peptide on *E. coli* HB101. Only relatively intact cells were imaged, and the images therefore represent only cells with minimal lytic damage at a particular peptide concentration. Because drying is part of the cell preparation procedure, there is a local change in peptide concentration, and this increase in peptide concentration may in effect

cause the damage to an unaffected cell or increase the damage to an already affected cell. We, however, did find that the concentration correlated well with cellular damage. In general, the roughness of the outer membrane increased with the increase in peptide concentration, with melittin having the most pronounced effect on the surface roughness. However, the most significant differences in cell morphology changes were dependent on the particular peptide and not so much on the peptide concentration. Representative images of cells and the damage to them by the respective peptides are discussed hereafter in detail.

Melittin at a concentration less than its LC_{50} induced structural changes in the bacterial cell wall. This resulted in the formation of grooves and pore-like lesions as well as the collapse of the cell structure at the apical ends. Figure 2A and B shows the topography and phase images of an *E. coli* cell treated with melittin at a concentration less than its LC_{50}. Both apical ends are collapsed and flattened, with the one end being more elastic or consisting of softer structures (see the encircled white area in Fig. 2B). Apart from the lesions, a large amount of released vesicles or peptide aggregates (which may include lipopolysaccharide [LPS] and membrane-associated compounds) with a diameter of 49.2 ± 10.9 nm are clearly visible around the cell in the phase image (Fig. 2B). Figure 2C is a magnification of a part of the cell surface. It shows pore-like lesions (65.7 ± 7.9 nm) and grooves (dark areas) on the surface. The surface corrugation was increased to 3.7 ± 1.43 nm (a >150% increase). As expected, a concentration of melittin greater than the LC_{50} leads to even greater cell damage of the *E. coli* cell, as is evident in the topography and phase images in Fig. 3A and B. In addition to a collapse of the apical ends, the outer membrane showed severe damage with large lesions of 87.5 ± 12.9 nm in diameter (Fig. 3C is a magnification of the cell surface). In both the topology and the phase images (Fig. 3A and B, respectively), the leakage of a substantial amount of fluid during the drying process is indicated by the "ring" around the cell. The "ring" phenomena around the cells were observed for a number of peptide-damaged cells. AFM images of droplets containing biological salts and small compounds show similar ring shapes after drying. Furthermore, the phase-contrast image of the visualized cell revealed possible blebbing at one of the apical ends (encircled in Fig. 3B). We found similar protrusions for *E. coli* cells treated with melittin in an earlier AFM study with a lower-resolution AFM instrument. The surface corrugation also increased to 7.72 ± 5.1 nm (a >300% increase), indicating a pronounced cell surface perturbation.

The effect of magainin 2a on *E. coli* was found to be quite different from that of melittin, although the concentration of compound that caused 50% inhibition of growth was virtually the same for these two peptides for *E. coli* by a microdilution assay (8). Figure 4A and B shows the topography and phase image, respectively, of a magainin 2a-treated *E. coli* cell. At the low concentrations, Mag 2a induced "surface-bound vesiculation" of the LPS-rich outer membrane with a "protovesicle" diameter of 51.5 ± 7.8 nm (see Fig. 4C for a magnification of the surface). Some lesions the size of protovesicles (49.2 ± 5.5 nm) can also be seen in the encircled areas of Fig. 4C. Electron microscopy studies by Matsuzaki et al. (18) showed similar results of vesicle formation by magainin 2. The phase image shows softer structures at one of the apical ends of the visualized cell (encircled white area in Fig. 4B). The surface corrugation increased by more than 370% to 9.1 ± 5.37 nm, which is comparable to that caused by melittin.

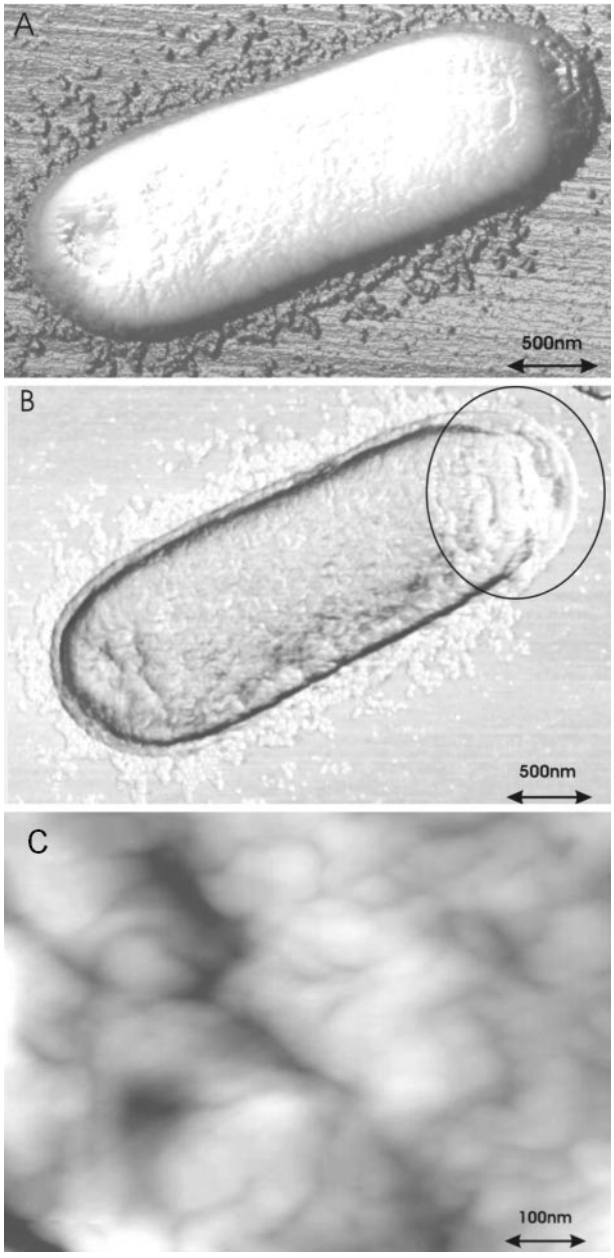

FIG. 2. (A) Topography image and (B) phase image of an *E. coli* cell treated with melittin at a concentration less than the LC_{50}; (C) magnification of the surface. The *z* scale ranges from 0 to 1.2 μm in panel A and from 0 to 50° in panel B. See the text for an explanation of the encircled area.

At a concentration greater than the LC_{50}, Mag 2a caused almost complete destruction of the bacterial cell. Figure 5A and B shows the topography and phase image, respectively, of Mag 2a-treated *E. coli* cells. Vesiculation, as well as deep lesions, can be observed, and the apical ends and the septal region of the cell are collapsed. It is also clearly visible in the

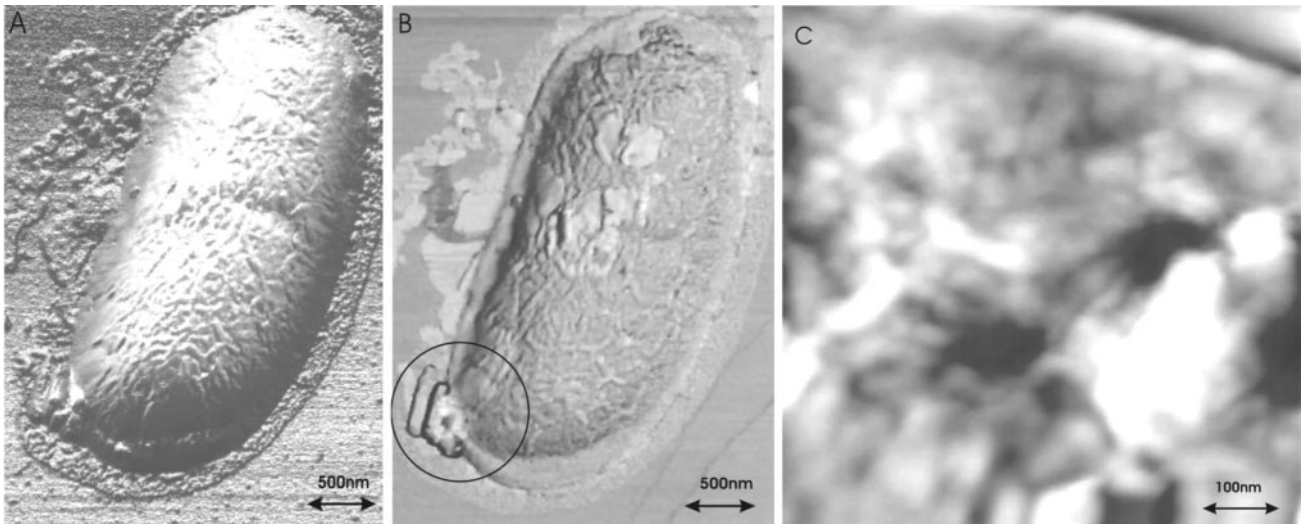

FIG. 3. (A) Topography image and (B) phase image of an *E. coli* cell treated with melittin at a concentration greater than the LC_{50}; (C) magnification of the surface. The *z* scale ranges from 0 to 0.8 μm in panel A and from 0 to 30° in panel B. See the text for an explanation of the encircled area.

phase image (Fig. 5B) that the inner membrane structures and remaining cellular contents have pulled away from the outer surface on the one side of the visualized cell. The outer surface here most probably consists mostly of the rigid peptidoglycan layer (Fig. 5C; see explanation below). Furthermore, both collapsed (flat circles) and intact vesicles with an average diameter of 50.4 ± 9.5 nm (excluding the larger vesicles and structures) can be seen in the phase image (Fig. 5B). The rod-like structures attached to the *E. coli* cell may possibly be magainin 2a filaments, as magainin 2 has been shown to spontaneously self-assemble into filaments in an ionic environment (27). Figure 5C is a magnification of the cell surface and shows deep lesions in the form of grooves and fewer vesicles than the number attained with the low Mag 2a concentration. The magnification of the surface indicates outer membrane thinning and the possible exposure of parts of the more rigid peptidoglycan layer, as indicated in Fig. 5D (encircled area). The surface corrugation increased by more than 280% to 6.95 ± 4.86 nm but decreased from that measured after the use of the lower Mag 2a concentration.

PGLa was found to be more active in terms of growth inhibition than Mag 2a, but it caused less visual damage to the *E. coli* cells that we examined (17.3 ± 1.04 mM of Mag 2a and 5.5 ± 1.0 mM of PGLa were needed to cause 50% growth inhibition, as measured by the Du Toit and Rautenbach assay [8]). The morphological change to the outer cell membrane of *E. coli* induced by low concentrations of PGLa can be described as intermediate between the changes induced by melittin and Mag 2a. Figure 6A and B shows the topography and phase images of two PGLa-treated *E. coli* cells, respectively. PGLa

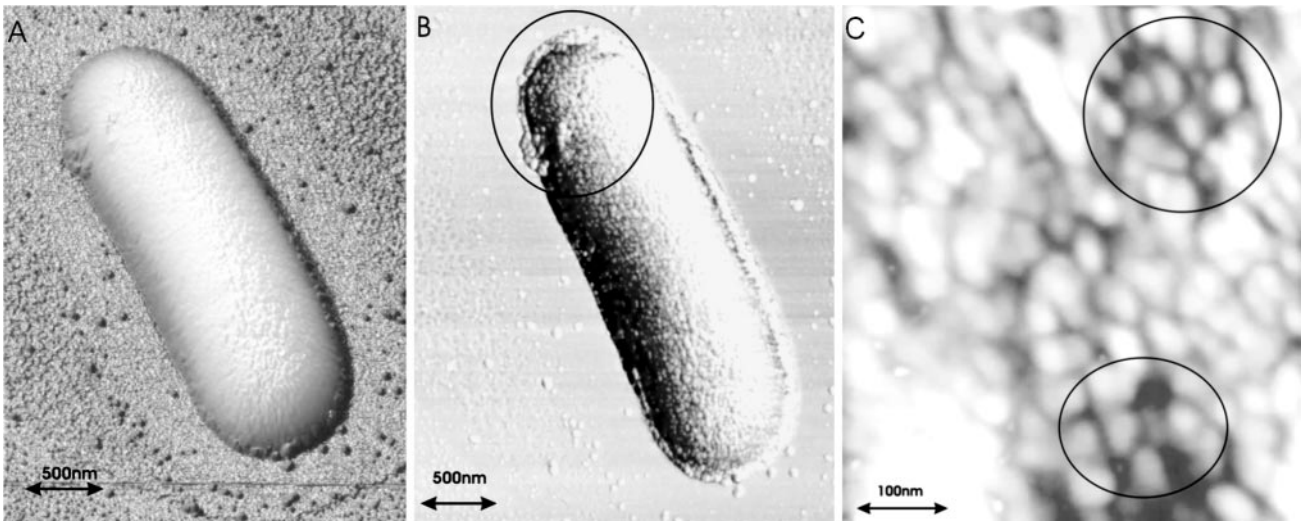

FIG. 4. (A) Topography image and (B) phase image of an *E. coli* cell treated with Mag 2a at a concentration less than the LC_{50}; (C) magnification of the surface. The *z* scale ranges from 0 to 0.8 μm in A and from 0 to 90° in panel B. See the text for an explanation of the encircled areas.

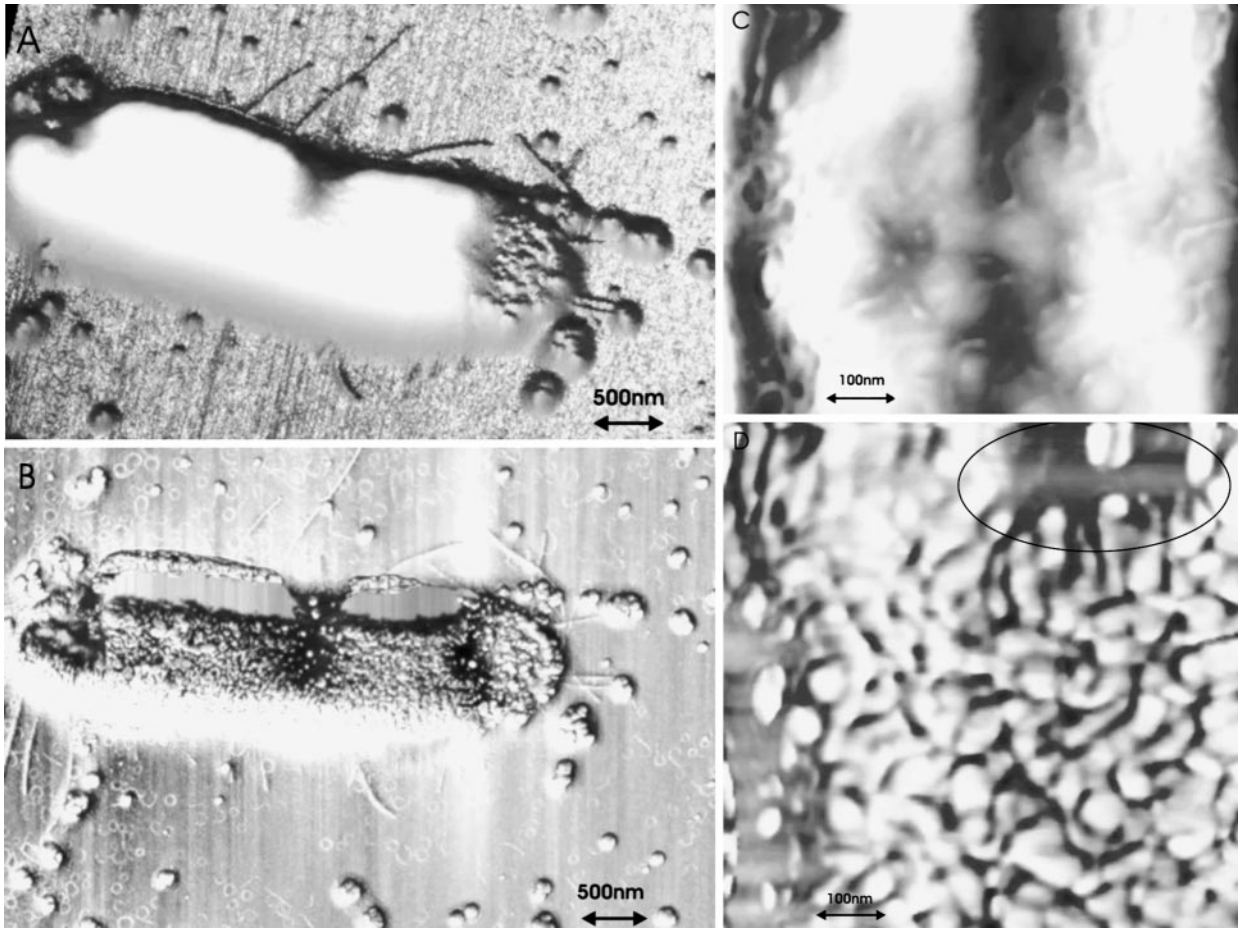

FIG. 5. (A) Topography image and (B) phase image of an *E. coli* cell treated with Mag 2a at a concentration greater than the LC_{50}; (C) magnification of the surface; (D) phase image of the magnified surface. The *z* scale ranges from 0 to 0.8 μm in panel A and from 0 to 80° in panel B. See the text for an explanation of the encircled area.

caused striations with an almost vesicle-like appearance, as well as some larger cell lesions with a size of 113.8 ± 37 nm (Fig. 6C) that may have been the cause of damage of areas in the cell capsule and the apical ends (Fig. 6A and B). The slight collapse (damage) of the apical ends and the center of the cell and the lesions across the entire surface become visible, especially in the phase image. The surface corrugation was only slightly increased by >110% to 2.83 ± 1.03 nm.

Figure 7A and B shows the topography and phase images of an *E. coli* cell treated with PGLa at a concentration greater than the $LC_{50.}$ At this higher PGLa concentration, the striations were more pronounced, although the cellular outer structure remained intact (Fig. 7A). The striations are dispersed between long and narrow lesions and grooves (Fig. 7C). The "ring" around the images in Fig. 7A and B indicates that cytosolic fluids leaked from the cell during the drying process (see the explanation above for Fig. 3A and B). The phase image shows the pronounced collapse of some of the inner structures of the cell (similar to that caused by Mag 2a), in particular, in the center of the cell. Softer structures at the apical ends are indicated by the white parts in the phase image (Fig. 7B). The surface roughness increased only by about 140% to 3.46 ± 0.7 nm. It seems as if the higher concentration of PGLa causes grooves and outer membrane-associated protovesicles with a diameter of 32.7 ± 5.5 nm. This is more like the vesicle-like structures caused by Mag 2a rather than the large lesions caused by melittin.

DISCUSSION

As with other microscopy techniques, we could visualize only those cells that remained relatively intact after the initial peptide action. Many of these cells may well be the most resistant cells in our cell cultures, specifically, in samples with a high peptide concentration, in which intact cells were a rare occurrence. However, some sensitive cells may have remained intact at the low peptide concentrations used and were possibly visualized. Also, due to concentration of the peptide during the drying step before visualization, many, if not most, of the surviving cells were ultimately damaged. This AFM study revealed intricate details of the membranolytic effects of three antimicrobial peptides on the cell envelope and, in particular, the LPS-rich outer membrane of these *E. coli* cells.

All the peptides caused an increase in surface roughness and lesions in the bacterial cell wall as a result of peptide treatment, with Mag 2a and melittin causing greater increases than

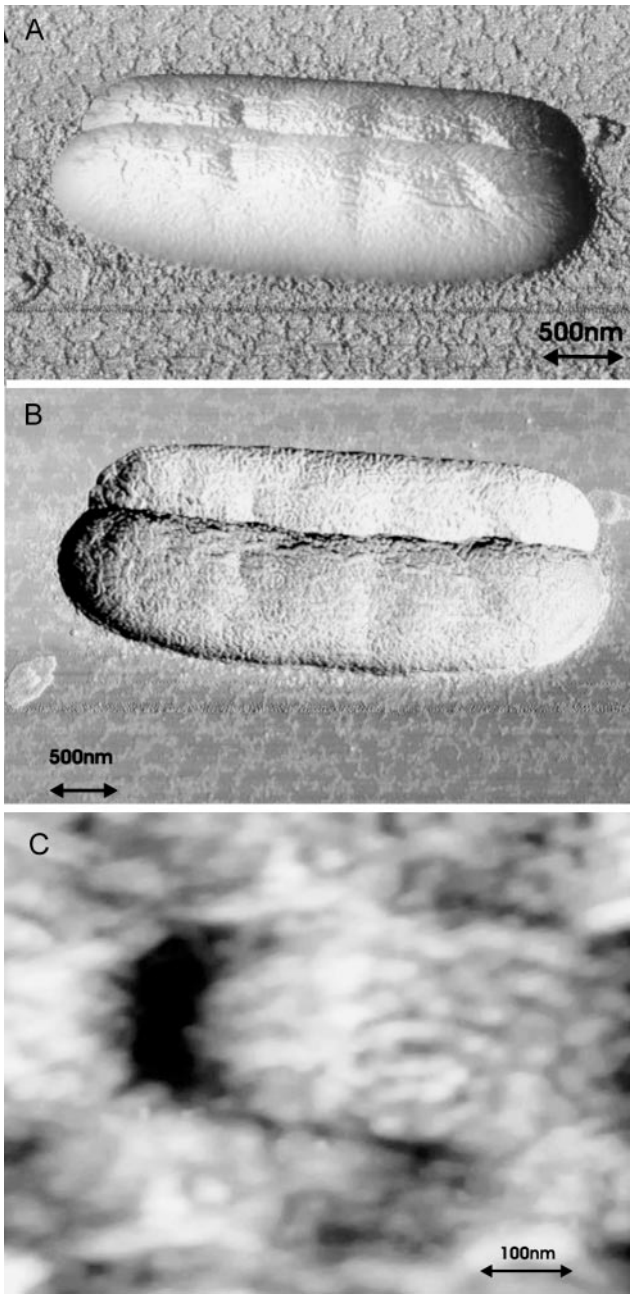

FIG. 6. (A) Topography image and (B) phase image of two *E. coli* cells treated with PGLa at a concentration less than the LC_{50}; (C) magnification of the surface. The *z* scale ranges from 0 to 0.8 μm in panel A and from 0 to 70° in panel B.

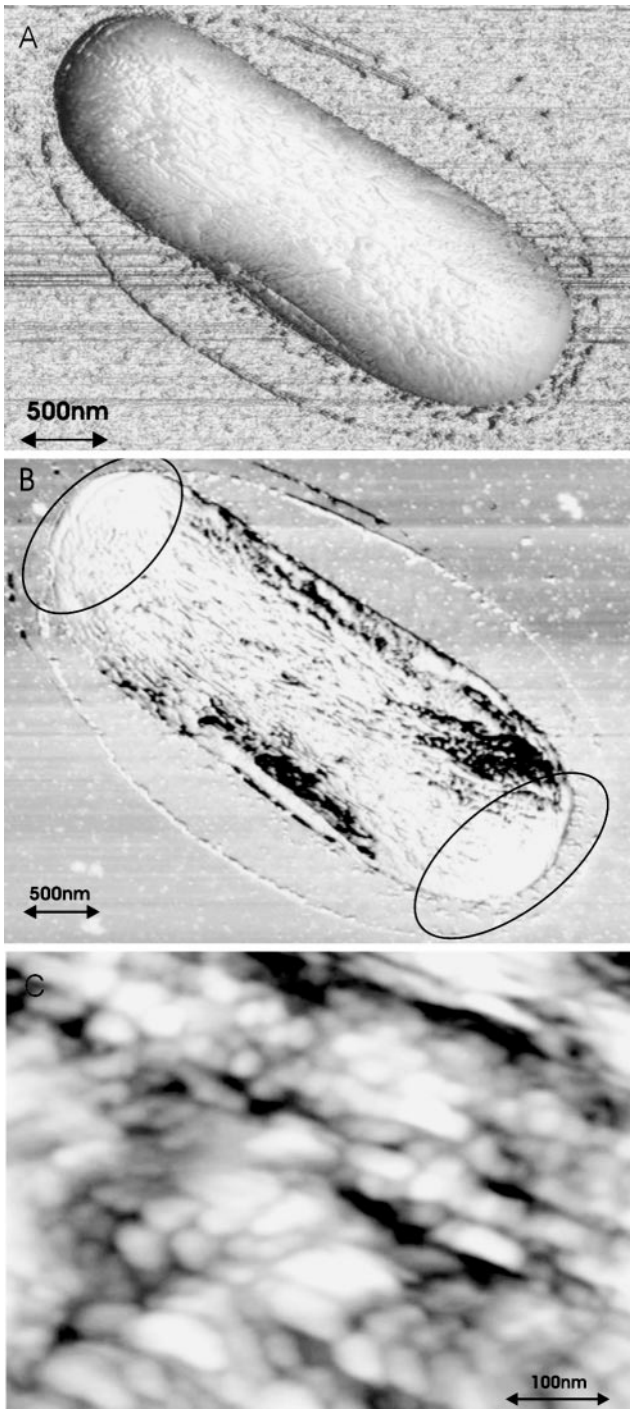

FIG. 7. (A) Topography image and (B) phase image of an *E. coli* cell treated with PGLa at a concentration greater than the LC_{50}; (C) magnification of the surface. The *z* scale ranges from 0 to 0.8 μm in panel A and from 0 to 120° in panel B. See text for explanation on encircled areas.

PGLa. The increase in surface roughness may have been caused by peptide incorporation into the LPS-containing outer membrane (7, 17), causing a "crumpling" effect due to an increase in surface area. The lesions may have been caused by either peptide aggregates (19, 30), the release of LPS-containing vesicles (17), or even autolytic reactions (1, 9). It has been shown by Matsuzaki et al. (17) that an analogue of magainin 2 preferentially interacted with LPS-containing vesicles rather than phosphatidylcholine-containing vesicles. Our AFM results clearly show that the LPS-rich outer membrane of the gram-negative bacterium *E. coli* is an important target for antimicrobial peptides. Our results therefore also support the finding of Ding et al. (7) that magainin has a transmembrane penetrating ability in LPS bilayers. The damage to the outer membrane may in turn improve the uptake of peptide to the

highly sensitive inner membrane (self-promoted uptake). Damage to the inner membrane will lead to leakage of the cytosol and eventual lysis and cell death.

Many of our phase-contrast images showed softer and more elastic structures at one or both of the apical ends (see the encircled white areas in Fig. 2B, 3B, 4B, and 7B). This indicates either a protrusion of the softer, more elastic inner membrane through lesions in the more rigid peptidoglycan layer or an accumulation of aggregates and/or vesicles at the apical end (Fig. 2B). All three peptides tended to induce the most damage at the apical ends of the cells. This result corresponds well with the results from an experiment with a cardiolipin-specific fluorescent dye where domains of cardiolipin (a negative phospholipid) were located, apart from at the septal regions, at the apical ends of the *E. coli* inner membrane (21). The three peptides evaluated in our study are highly cationic and have a higher affinity for negative phospholipids than for neutral phospholipids (13, 22). Therefore, it is possible that a higher concentration of peptide will be trapped at the apical ends. The damage at the apical ends is probably the consequence of inner membrane damage rather than outer membrane damage.

Apart from the similarities discussed above, the overall effects of the three peptides on the cell envelope and the cell were observed to be different in some aspects. Melittin caused large lesions in the cell envelope and also pronounced leakage of cytosolic fluid, which indicates damage to the inner membrane. If the lesions and released vesicles (or membrane component-peptide aggregates) are an indication of melittin's mechanism of action on the outer membrane, these results suggest that melittin utilized a carpet (23) or micelle-aggregate (19, 30) mechanism (both of which are detergent-like) on the negative LPS-containing outer membrane. Ladokhin and White (14) as well as Papo and Shai (24) suggested that melittin permeabilized anionic lipid vesicles in a "detergent-like" fashion. However, it is not clear which part of the damaged cell, the inner membrane or the outer membrane, plays the most important role in the eventual lytic action of melittin.

It was clearly demonstrated by our AFM results that Mag 2a causes pronounced vesiculation of the outer membrane. In particular, the almost 100% decrease in surface roughness from the low to high Mag 2a concentrations and the exposure of rigid areas in the cell wall (Fig. 5) indicated that some components were released from the cell envelope, possibly by vesiculation. This strongly indicates carpeting of the outer LPS-containing membrane (and vesicle release), as suggested by Oren and Shai (23) from their studies with model membranes.

The mechanism of action of PGLa is still unclear, but it does correlate somewhat with that of magainin in the way in which it promotes the formation of small outer membrane protovesicles. However, although PGLa also caused a positive increase in the curvature of the outer membrane (protovesicles), the higher PGLa concentrations did not cause a massive release of vesicles like that seen with magainin 2a. The fact that the cell surface roughness increase was much less with PGLa than with the other two peptides may point to limited carpeting and surface expansion but a sufficient interaction with the outer membrane so that small lesions are formed. These lesions could be the gateway to the self-promoted uptake of the highly active PGLa to the more sensitive inner membrane.

Conclusion. This is the first visual demonstration of the actual effect of antimicrobial peptides on living bacterial cells. In summary, the results from this AFM study proved that it is possible to distinguish between the types of damage to the outer membrane of gram-negative bacterial cells caused by different peptides.

ACKNOWLEDGMENTS

The Veeco Multimode scanning probe microscope is a loan from the Center for Macromolecular Chemistry and Technology in Tripoli, Libya.

The BIOPEP Peptide Group, the National Research Foundation (NRF), and the Technology and Human Resources for Industry Programme (THRIP) of South Africa provided funding for this project.

REFERENCES

1. **Bierbaum, G., and H. G. Sahl.** 1985. Induction of autolysis of staphylococci by the basic peptide antibiotics Pep 5 and nisin and their influence on the activity of autolytic enzymes. Arch. Microbiol. **141:**249–254.
2. **Boheim, G.** 1974. Statistical analysis of alamethicin channels in black lipid membranes. J. Membr. Biol. **19:**277–303.
3. **Bonomo, R. A.** 2000. Multiple antibiotic-resistant bacteria in long-term-care facilities: an emerging problem in the practice of infectious diseases. Clin. Infect. Dis. **31:**1414–1422.
4. **Braga, P. C., and D. Ricci.** 1998. Atomic force microscopy: application to investigation of *Escherichia coli* morphology before and after exposure to cefodizime. Antimicrob. Agents Chemother. **42:**18–22.
5. **Dathe, M., and T. Wieprecht.** 1999. Structural features of helical antimicrobial peptides: their potential to modulate activity on model membranes and biological cells. Biochim. Biophys. Acta **1462:**71–87.
6. **Dempsey, C. E.** 1990. The actions of melittin on membranes. Biochim. Biophys. Acta **1031:**143–161.
7. **Ding, L., L. Yang, T. M. Weiss, A. J. Waring, R. I. Lehrer, and H. W. Huang.** 2003. Interaction of antimicrobial peptides with lipopolysaccharides. Biochemistry **42:**12251–12259.
8. **Du Toit, E. A., and M. Rautenbach.** 2000. A sensitive standardized micro-gel well diffusion assay for the determination of antimicrobial activity. J. Microbiol. Methods **42:**159–165.
9. **Galvez, A., E. Valdivia, M. Martinez-Bueno, and M. Maqueda.** 1990. Induction of autolysis in *Enterococcus faecalis* S-47 by peptide AS-48. J. Appl. Bacteriol. **69:**406–413.
10. **Garrett, R. H., and C. M. Grisham.** 2002. Biochemistry, 2nd ed., p. 32. Saunders College Publishing, Harcourt Brace College Publishers, Orlando, Fla.
11. **Habermann, E.** 1972. Bee and wasp venoms. Science **177:**314–322.
12. **Hancock, R. E. W.** 1999. Peptide antibiotics. Lancet **349:**418–422.
13. **Konovalov, O., I. Myagkov, B., Struth, and K. Lohner.** 2002. Lipid discrimination in phospholipid monolayers by the antimicrobial frog skin peptide PGLa. A synchrotron X-ray grazing incidence and reflectivity study. Eur. Biophys. J. **31:**428–437.
14. **Ladokhin, A. S., and S. H. White.** 2001. 'Detergent-like' permeabilization of anionic lipid vesicles by melittin. Biochim. Biophys. Acta **1514:**253–260.
15. **Liu, P., Y. Liu, Z. Lu, J. Zhu, J. Dong, D. Pang, P. Shen, and S. Qu.** 2004. Study on biological effect of La^{3+} on *Escherichia coli* by atomic force microscopy. J. Inorg. Biochem. **98:**68–72.
16. **Ludtke, S. J., K. He, W. T. Heller, T. A Harroun, L. Yang, and H. W. Huang.** 1996. Membrane pores induced by magainin. Biochemistry **35:**13723–13728.
17. **Matsuzaki, K., K. Sugishita, and K. Miyajima.** 1999. Interactions of an antimicrobial peptide, magainin 2, with lipopolysaccharide-containing liposomes as a model for outer membranes of gram-negative bacteria. FEBS Lett. **449:**221–224.
18. **Matsuzaki, K., K. Sugishita, M. Harada, N. Fujii, and M. Miyajima.** 1997. Interactions of an antimicrobial peptide, magainin 2, with outer and inner membranes of gram-negative bacteria. Biochim. Biophys. Acta **1327:**19–130.
19. **Matsuzaki, K., O. Murase, H. Tokuda, S. Funakoshi, N. Fujii, and K. Miyajima.** 1994. Orientational and aggregational states of magainin 2 in phospholipid bilayers. Biochemistry **33:**3342–3349.
20. **Matsuzaki, K., O. Murase, N. Fujii, and K. Miyajima.** 1996. An antimicrobial peptide, magainin 2, induced rapid flip-flop of phospholipids coupled with pore formation and peptide translocation. Biochemistry **35:**11361–11368.
21. **Mileykovskaya, E., and W. Dowhan.** 2000. Visualization of phospholipid domains in *Escherichia coli* by using the cardiolipin-specific fluorescent dye 10-*N*-nonyl acridine orange. J. Bacteriol. **182:**1172–1175.
22. **Mozsolits, H., H. J. Wirth, J. Werkmeister, and M. I. Aguilar.** 2001. Analysis

of antimicrobial peptide interactions with hybrid bilayer membrane systems using surface plasmon resonance. Biochim. Biophys. Acta **1512:**64–76.
23. **Oren, Z., and Y. Shai.** 1998. Mode of action of linear amphipathic alpha-helical antimicrobial peptides. Biopolymers **47:**451–463.
24. **Papo, N., and Y. Shai.** 2003. Exploring peptide membrane interaction using surface plasmon resonance: differentiation between pore formation versus membrane disruption by lytic peptides. Biochemistry **42:**458–466.
25. **Rautenbach, M., and J. W. Hastings.** 1999. Cationic peptides with antimicrobial activity—the new generation of antibiotics? Chim. Oggi/Chem. Today Nov./Dec.:81–89.
26. **Sharma, S., P. Sen, S. N. Mukhopadhyay, and S. K. Guha.** 2003. Microbicidal male contraceptive—Risug induced morphostructral damage in *E. coli*. Colloids Surfaces B **32:**43–50.
27. **Urrutia, R., R. A. Cruciani, J. L. Barker, and B. Kachar.** 1989. Spontaneous polymerization of the antibiotic peptide magainin 2. FEBS Lett. **247:**17–21.
28. **Westerhoff, H. V., M. Zasloff, J. L. Rosner, R. W. Hendler, A. De Waal, V. A. Gomes, P. M. Jongsma, A. Riethorst, and D. Juretic.** 1995. Functional synergism of the magainins PGLa and magainin-2 in *Escherichia coli*, tumor cells and liposomes. Eur. J. Biochem. **228:**257–264.
29. **Wong, A. H., R. P. Wenzel, and M. B. Edmond.** 2000. Epidemiology of bacteriuria caused by vancomycin-resistant enterococci—a retrospective study. Am. J. Infect. Control **28:**277–281.
30. **Wu, M., E. Maier, R. Benz, and R. E. W. Hancock.** 1999. Mechanism of interaction of different classes of cationic antimicrobial peptides with planar bilayers and with the cytoplasmic membrane of *Escherichia coli*. Biochemistry **38:**7235–7242.
31. **Yang, L., T. A. Harroun, T. M. Weiss, L. Ding, and H. W. Huang.** 2001. Barrel-stave model or toroidal model? A case study on melittin pores. Biophys. J. **81:**1475–1485.
32. **Zasloff, M.** 1987. Magainins, a class of antimicrobial peptides from *Xenopus* skin: isolation, characterization of two active forms, and partial cDNA sequence of a precursor. Proc. Natl. Acad. Sci. USA **84:**5449–5453.
33. **Zasloff, M., B. Martin, and H. C. Chen.** 1988. Antimicrobial activity of synthetic magainin peptides and several analogues Proc. Natl. Acad. Sci. USA **85:**910–913.